NY-08-057

Thermal Resistance of a Window with an Enclosed Venetian Blind: A Simplified Model

John L. Wright, PhD
Member ASHRAE

Michael R. Collins, PhD
Associate Member ASHRAE

Ned Y.T. Huang

ABSTRACT

Solar gain has a strong influence on building energy consumption and peak cooling load. Venetian blinds are routinely used to control solar gain. Software based on 1-D models is available to accurately predict the thermal performance of glazing systems but the development of models for shading devices is at a very early stage. An accurate model has been formulated to quantify the thermal resistance of a glazing system with an enclosed venetian blind. It is possible to account for pane spacing, slat angle, alternate fill gases and the presence of a low-emissivity coating. Effective longwave optical properties are assigned to the blind layer in order to calculate radiant heat transfer. An exceptionally simple model for convective heat transfer, the reduced slat length (RSL) model, has been developed on the basis of guarded heater plate measurements. CFD results reveal reasons for the very close agreement between measurement and the RSL model. The new simulation capability can be applied to the quantification of U-factor and Solar Heat Gain Coefficient. The simplicity of the RSL model is particularly valuable in the context of building energy simulation where CPU time must be used sparingly.

INTRODUCTION

Background

Window area, and its associated design, distribution, orientation, etc., effect solar gain and heat losses of a building. Proper fenestration design can greatly reduce unwanted energy gains/losses and can help maintain a comfortable indoor space. Solar gain is of particular importance because of both its magnitude and variability. Shading devices such as venetian blinds, roller blinds and drapes are frequently used to control solar gain. Therefore, the current effort to create models for shaded windows is expected to be of significant value—especially in the field of computational building loads and energy analysis.

One-dimensional (1-D) centre-glass models have been developed (e.g., Finlayson 1993; Hollands et al. 2001; Hollands and Wright 1983; Wright 1980, 1998; Rubin 1982; Van Dijk and Goulding 1996) to predict the thermal performance of glazing systems and these models are known to be accurate (e.g., Carpenter 1992; Wright and Sullivan 1987, 1988). Software based on these models is widely used for design, code compliance and rating. In contrast, the development of models for windows with shading devices is at a very early stage. One set of shading layer models is available (Van Dijk and Goulding 1996) but the user is required to quantify the air permeability of certain types of shading layers with little guidance except for the instruction that the appropriate value is to be determined by means of experiment or computational fluid dynamics (CFD) modelling.

Overview of this Study

The problem of interest and some of the nomenclature are shown in Figure 1. A venetian blind is positioned at the centre of a vertical glazing cavity. The temperature difference between the two glazing surfaces drives heat transfer across the cavity. The radiant and convective heat transfer components are coupled because of the presence of the venetian blind. The goal of this research was to formulate a model to quantify this coupled heat transfer. The resulting model is based on guarded heater plate (GHP) measurements. Parallel studies, based on CFD modelling of the natural convection, provide insights regarding the flow field (Tasnim 2005, Naylor
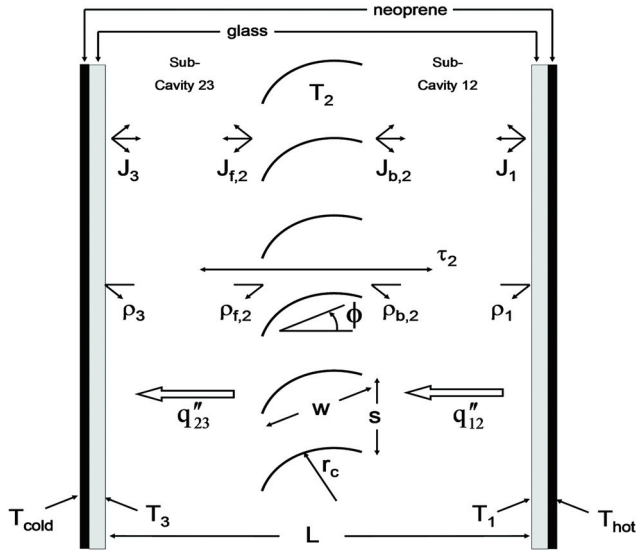
Figure 1 *Heat transfer across a glazing cavity with an internal venetian blind.*

Figure 2 *Guarded heater plate measurements (Huang 2005, Huang et al. 2006)*
Note: Divide U-factor by 5.678 to obtain IP units ($Btu/h \cdot ft^2 \cdot °F$).

and Collins 2005) that support the validity of the model. The radiant exchange component of the model was described by Yahoda and Wright (2004a, 2004b).

Measured Data

Two sets of guarded heater plate measurements are available for the configuration described in the previous paragraph (Garnet et al. 1995, Garnet 1999, Huang 2005, Huang et al. 2006). Garnet measured center-glass heat transfer rates across a cavity bounded by uncoated glass and containing a venetian blind comprised of painted aluminum slats. Huang used the same apparatus to reproduce the measurements of Garnet and extended the range of variables—most notably by examining the presence of a low emissivity (low-e) coating on one of the glass surfaces. In each instance measurements were obtained by placing the test sample, consisting of two glass layers and the enclosed venetian blind, between two copper plates that were maintained at fixed temperatures (T_{hot} and T_{cold}) by two constant temperature baths. Thin neoprene mats were placed between the copper and glass surfaces to eliminate contact resistance. These mats are shown in Figure 1 as heavy black lines.

The GHP measurements of Huang et al. (2006) are presented in Figure 2. The upper group of data corresponds to samples with uncoated glass and the lower group corresponds to systems that included a low-e coating. Each group includes data for three pane spacings (L = 17.78, 25.4 and 40.01 mm (L = 0.7, 1.0 and 1.575 in.). The venetian blind was a commercially produced product with painted aluminum slats (w = 14.79 mm (w =0.582 in.), s =11.84 mm (s = 0.466 in.), $r_c/w \approx 2$). The hemispheric emissivity of the painted slat surfaces was ε_{slat} = 0.792 (Yahoda and Wright 2004b). The
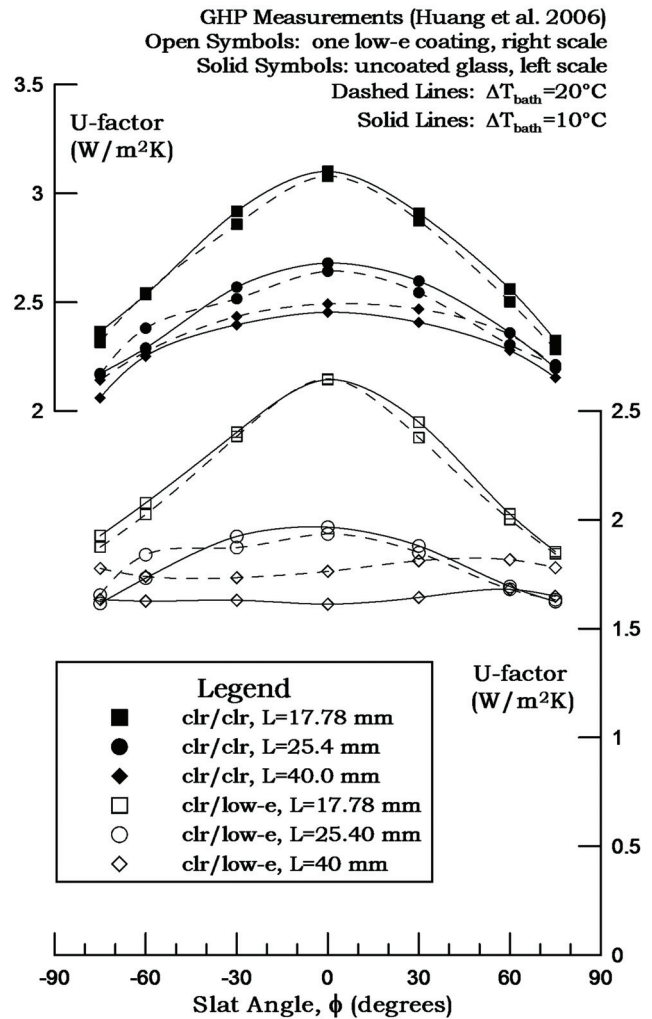
hemispheric emissivity of the low-e surface was reported by Huang et al. (2006) as ε_{low-e} = 0.164 and the emissivity of uncoated glass is known to be ε_{gl} = 0.84.

It is important to make a note about pane spacing at this stage. All three pane spacings used by Garnet [L = 17.78, 20.32 and 25.4 mm (0.7, 1.0, 1.575 in.)] and the two small pane spacings used by Huang (L = 17.78 and 25.4 mm [0.7, 1.0, 1.575 in.)] were chosen to include the full range of spacings likely to be found in a commercially produced product. The measurements of Huang, used for comparison in this study, included a much larger pane spacing [L = 40.01 mm (1.575 in.)]. Huang et al. (2006) stated that this large spacing was not seen as a popular, or even likely, design option. It was studied for more fundamental reasons including the hope of obtaining approximate information about the smallest spacing at which slat angle and/or pane spacing itself have little or no effect on heat transfer. Therefore, greater priority was placed on comparison with the measurements made at

$L = 17.78$ mm (0.7 in.) and $L = 25.4$ mm (1.0 in.). Comparisons with measurements at $L = 40.01$ mm (1.575 in.) are also presented but this is done out of curiosity and for the sake of completeness. Results generated at this large pane spacing should be viewed with much less emphasis.

Each sample was tested twice; once with the constant temperature bath thermostats set to 30°C (86°F) and 20°C (68°F) [$\Delta T_{bath} = 10$°C (18°F)] and again with the cold bath setting lowered to 10°C (50°F) [$\Delta T_{bath} = 20$°C (36°F)]. The measured plate-to-plate temperature difference, $\Delta T_{pp} = T_{hot} - T_{cold}$, is always less than ΔT_{bath} and the difference between the two is influenced by the thermal resistance of the test sample itself. Nonetheless, the difference between ΔT_{bath} and ΔT_{pp} was small (less than 5% of ΔT_{pp} in almost all cases) so the two values of ΔT_{bath} used in the experiments can be viewed as nominal values of ΔT_{pp}.

It should be noted that the U-factors shown in Figure 2 were obtained by replacing the thermal resistance of the neoprene mats with fixed indoor and outdoor heat transfer coefficients, h_i and h_o. More specifically,

$$U_{meas} = \left(R_{tot} - 2R_n + \frac{1}{h_o} + \frac{1}{h_i} \right)^{-1} \quad (1)$$

where measured values of ΔT_{pp} and heat flux, q'', were used to obtain the total (i.e., plate-to-plate) thermal resistance of the sample-plus-mats assembly, R_{tot}.

$$R_{tot} = \frac{\Delta T_{pp}}{q''} \quad (2)$$

The combined resistance of the two neoprene mats, measured by Huang (2005), was

$$2R_n = 0.01 \frac{m^2 \cdot K}{W} = 0.0568 \frac{h \cdot ft^2 \cdot °F}{Btu} \quad (3)$$

Garnet (1999) and Huang (2005) chose to use fixed values of $h_i = 8.0$ W/m²·K (1.41 Btu/h·ft²·°F) and $h_o = 23.0$ W/m²·K (4.05 Btu/h·ft²·°F) and this choice is reflected in Figure 2.

HEAT TRANSFER MODEL

Model Structure

Several models were devised in an attempt to reproduce the GHP measurements of Huang. In each instance the focus of the model was the heat transfer within the glazing cavity.

Each model was based on a structure of three temperature nodes. These nodes correspond to the glass surface temperatures, T_1 and T_3, plus the temperature of the venetian blind, T_2. See Figure 1. A more sophisticated model might have been chosen, perhaps with two or more temperature nodes assigned to the venetian blind layer, but it was hoped that the simpler approach would be sufficient. The simplicity of a three-node model is especially useful in the context of building energy analysis software where CPU time must be used sparingly.

Boundary Conditions

The glass surface temperatures, T_1 and T_3, needed to complete each simulation were obtained using measured heat flux and plate temperatures from individual experiments.

$$T_1 = T_{hot} - (R_n + R_g)q'' \quad (4)$$

$$T_3 = T_{cold} - (R_n + R_g)q'' \quad (5)$$

where the thermal resistance of each glass layer was taken as:

$$R_g = 0.003 \frac{m^2 \cdot K}{W} = 0.017 \frac{h \cdot ft^2 \cdot °F}{Btu} \quad (6)$$

Calculation of U-Factor

U-factors produced by simulation models, U_{sim}, were compared to the GHP measurements shown in Figure 2. In each case the heat flux predicted by the simulation, q''_{sim}, was converted to a U-factor using Equation (7).

$$U_{sim} = \left(\frac{T_1 - T_3}{q''_{sim}} + 2R_g + \frac{1}{h_o} + \frac{1}{h_i} \right)^{-1} \quad (7)$$

The mean temperatures in sub-cavities 12 and 23, $T_{m,12} = (T_1 + T_2)/2$ and $T_{m,23} = (T_2 + T_3)/2$, were used to determine the air properties in the two sub-cavities. The blind layer temperature, T_2, was determined by iteration and the air properties were updated at each step of the process.

The Radiant Exchange Model

The longwave optical properties of each component influence heat transfer across the cavity. At the glass surfaces the hemispheric emissivities are denoted ε_1 and ε_3. Glass is opaque with respect to longwave radiation so the longwave reflectivities of these surfaces are $\rho_1 = 1 - \varepsilon_1$ and $\rho_3 = 1 - \varepsilon_3$. The venetian blind was treated as a continuous, uniform layer by assigning it effective (i.e., spatially averaged) front-side and back-side longwave properties: $\varepsilon_{f,2}$, $\rho_{f,2}$, $\varepsilon_{b,2}$, $\rho_{b,2}$ and τ_2. This set of blind layer properties was evaluated, as a function of slat geometry and emissivity of the slat surfaces, using the four-surface/flat-slat model presented by Yahoda and Wright (2004a). The front-side and back-side effective properties of the blind layer do not differ ($\varepsilon_{f,2} = \varepsilon_{b,2}$ and $\rho_{f,2} = \rho_{b,2}$) because the two slat surfaces have the same properties. The effective blind-layer properties are presented as functions of slat angle in Figure 3.

The radiant mode of heat transfer was quantified in terms of the radiosities shown in Figure 1 (J_1, $J_{b,2}$, $J_{f,2}$, J_3). This method is well documented (e.g., Hollands et al. 2001, Hollands and Wright 1983, Rubin 1982, Yahoda and Wright 2004b). Each radiosity is simply the radiant flux leaving a surface—including emitted, reflected and transmitted components. The net radiant heat flux across either sub-cavity is just

Effective Longwave
Properties of
Venetian Blind
$\rho_{slat}=0.208$
$\tau_{slat}=zero$
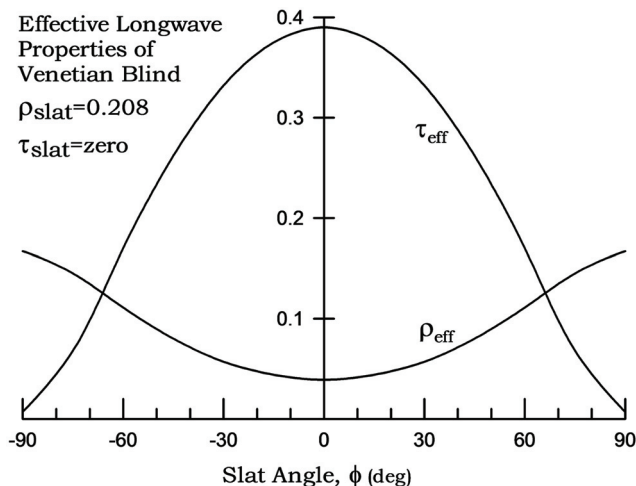
Figure 3 *Effective longwave properties of venetian blind layer.*

the difference between the radiosities of the bounding surfaces.

Note that each radiant flux is presumed to be diffuse and shape factors between adjacent layers are all equal to unity. The air is non-participating. Also note that $J_{f,2}$ and $J_{b,2}$ each include a transmitted flux component because the venetian blind will in general be partially transparent to longwave radiation:

Equations (8) through (11) describe the interaction between, and the components of, the various radiosities. These equations comprise a complete radiant exchange model for the system of interest.

$$J_1 = \varepsilon_1 \sigma T_1^4 + \rho_1 J_{b,2} \qquad (8)$$

$$J_{f,2} = \varepsilon_{f,2} \sigma T_2^4 + \rho_{f,2} J_3 + \tau_2 J_1 \qquad (9)$$

$$J_{b,2} = \varepsilon_{b,2} \sigma T_2^4 + \rho_{b,2} J_1 + \tau_2 J_3 \qquad (10)$$

$$J_3 = \varepsilon_3 \sigma T_3^4 + \rho_3 J_{f,2} \qquad (11)$$

If T_2 is known this system of equations can be solved by various methods including matrix reduction. The system is small enough to algebraically obtain explicit expressions for the four radiosities (Huang 2005).

Convective Heat Transfer

The various heat transfer models described in the following sections make use of a convective heat transfer coefficient, h, that is estimated using a correlation that applies to heat transfer across a tall, vertical, gas filled, rectangular cavity—such as a conventional glazing cavity. In each case, having chosen a characteristic length, x, the Nusselt number based on x, Nu_x, is calculated as a function of the Rayleigh number, Ra_x. The Rayleigh number is a function of the temperature difference across the cavity, several gas properties and the charac-

teristic length, x. In the case of a glazing cavity x is generally chosen to be the pane spacing. Equations (12) and (13) show some of the detail.

$$Ra_x = \frac{\rho^2 g \beta C_p \Delta T x^3}{\mu k} \qquad (12)$$

$$h = Nu_x \frac{k}{x} \qquad (13)$$

Air properties (specific heat at constant pressure C_p, dynamic viscosity μ, thermal conductivity k) were determined as a function of air temperature using regressions fitted to data (Hilsenrath 1955) over the temperature range from 283 K to 303 K. The air density, ρ, was determined using the ideal gas relationship. The compressibility factor was found to be within 1% of unity for all cases ($z = 0.995$ was used). The local value of acceleration due to gravity is $g = 9.8064$ m/s^2 ($g = 32.173$ ft/s^2) (Bolz and Tuve 2000). The thermal expansion coefficient is $\beta = 1/T_m$ for a perfect gas.

In this study the correlation of Wright (1996)* was used to evaluate the function $Nu_x = Nu(Ra_x)$ but any one of several similar correlations (e.g., Shewen et al. 1996, Elsherbiny et al. 1982) could have been used to obtain the same results.

Coupled Heat Transfer

Expressions for heat flux across each of the two subcavities can be written by considering the components of convective heat transfer and longwave radiant exchange:

$$q_{12}'' = h_{12}(T_1 - T_2) + J_1 - J_{b,2} \qquad (14)$$

$$q_{23}'' = h_{23}(T_2 - T_3) + J_{f,2} - J_3 \qquad (15)$$

If the convective heat transfer coefficients, h_{12} and h_{23}, are known Equations (8) to (11) plus (14) and (15) constitute a complete model for heat transfer across the cavity. The goal is to find T_2 such that $q_{12}'' = q_{23}''$ and since the convective heat transfer coefficients and radiosities are all influenced by T_2 the solution must be generated by iteration. The details of the solution algorithm are of little importance; any one of many techniques can be used.

NATURAL CONVECTION MODELS

Simple Natural Convection Model, M1

To establish a point of reference a relatively simple model for convective heat transfer (M1) is presented. This model is almost identical to one of the models examined by Yahoda and Wright (2004b) whose simulation results agreed only moderately well with measured data (Garnet et al. 1995)—generally within 10%. Similarly, in the current study model M1 did not perform well when compared to the measurements of Huang

---

*A correction: In (Wright 1996) the exponent in Equation 9b should be 0.41399 instead of 0.4134.

(Huang et al. 2006). Nonetheless, because this convection model does not include the influence of slat angle, it highlights the need to account for slat angle in more than just the radiation exchange and additional models are presented that explore that aspect of the problem.

Model M1 was devised by assuming that the venetian blind segregates the flow of the fill-gas as if there were two separate cavities. The heat transfer coefficients, h_{12} and h_{23}, were approximated using Nu_x determined separately for cavity 12 and cavity 23. In each case, x was set equal to half of the pane spacing ($x_{12} = x_{23} = L/2$). Yahoda and Wright (2004b) set the temperature difference across each sub-cavity equal to half of the temperature difference between hot and cold glazing ($T_{12} = T_{23} = (T_1 - T_3)/2$). In the present study the most recent estimate of T_2 was used ($T_{12} = T_1 - T_2$ and $T_{23} = T_2 - T_3$) at each iteration of the solution process. No thermal resistance was assigned to the venetian blind layer.

Figure 4 includes a comparison of model M1 versus GHP measurements for one particular test sample ($L = 17.78$ mm (0.7 in.), $\Delta T_{bath} = 20°C$ (68°F), low-e coating present). U-factors are shown as a function of slat angle, ϕ. This simple model agrees closely with measurement when the blind is fully closed (extrapolating the measurements to $\phi = \pm 90°$), as might be expected, but it does not account for the variation of ϕ as the slats are opened.

An important observation regarding Figure 4 is that the M1 model shows so little variation with ϕ. The convection component of the M1 model is not influenced by ϕ. Therefore, ϕ influences the M1 results only through changes in the effective optical properties of the blind layer and the resulting change in radiant heat transfer. In this case some of insensitivity with respect to ϕ will be due to the presence of the low-e coating. Assuming that the radiation model is accurate, an assertion supported by the close agreement at $\phi = \pm 90°$, it can be concluded that the influence of ϕ on the heat transfer across the cavity arises largely through its influence on convective heat transfer.

Tip-to-Glass Natural Convection Model, TG

A second model, TG, was devised by again assuming that the venetian blind segregates the glazing cavity in two cavities. This model is identical to model M1 except that in this case the width of each cavity was taken to be the distance from the tip of the blind slats to the adjacent glass surface [$x_{12} = x_{23} = (L - w \cdot \cos\phi)/2$]. Again, no thermal resistance was assigned to the venetian blind layer.

A comparison between model TG and GHP data is also shown in Figure 4. Again simulation and measurement approach each other as the blind is closed, and the slat angle clearly has an influence on calculated U-factors but this influence is far too strong. At this stage a third model was devised.

Reduced Slat Length Model, RSL

The TG convection model was modified in order to reduce its sensitivity to slat angle. This was accomplished by
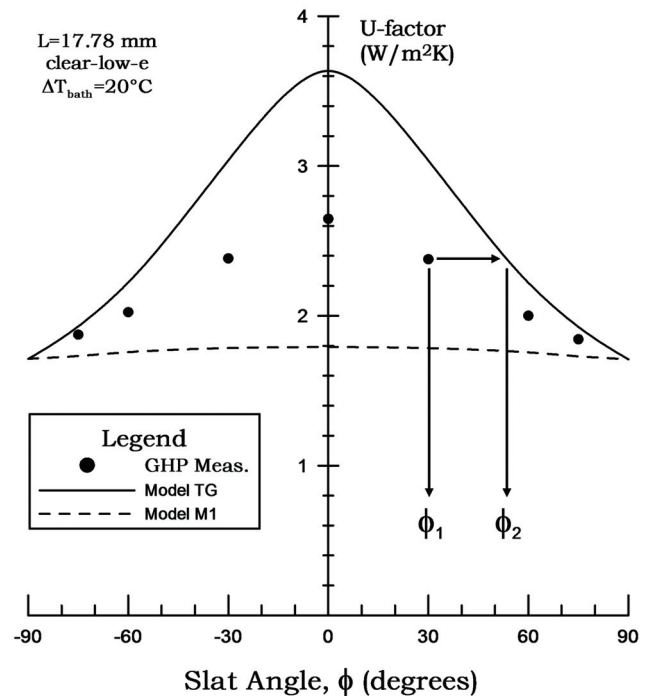
Figure 4 Typical U-factor versus slat angle plot: GHP results of Huang (2005) versus models M1 and TG.

introducing a factor, N, by which the slat width, w, would be reduced - solely for the purpose of determining an "effective" width of the tip-to-glass cavities.

$$x_{12} = x_{23} = \frac{L - N \cdot w \cdot \cos\phi}{2} \qquad (16)$$

The consequence of the reduced slat width is that the calculated U-factor remains unchanged when the blind is fully closed but at slat angles other than $\phi = \pm 90°$ the resistances of cavity 12 and cavity 23 increase because x_{12} and x_{23} increase as the slats are shortened. The effect of this modification is greatest when the blind is fully open ($\phi = 0$), as desired. Note that the slat width remains unaltered in the radiant exchange portion of the model.

It was possible to evaluate N graphically. Consider one of the GHP measurements shown in Figure 4, say at $\phi = \phi_1$. For each value of ϕ_1 there is a corresponding slat angle ϕ_2 at which the TG model predicts the correct U-factor for the ϕ_1 geometry. Ignoring the change in radiant heat transfer, an expression for N can be obtained by comparing the two cases.

$$N = \frac{\cos\phi_2}{\cos\phi_1} \qquad (17)$$

Equation (17) was applied to the data for $L = 17.78$ mm (0.7 in.) and $L = 25.40$ mm (1.0 in.). The consistent outcome was remarkably simple: $N \approx 0.7$. The RSL model, with $N = 0.7$, was used to calculate U-factors for all of the GHP test

conditions. The results are listed as U_{sim} in Tables 1, 2 and 3. Evidence of radiant coupling can be seen in the temperature of the venetian blind, T_2, which is several degrees lower when a low-e coating is present on the warm glazing. Curves (cubic spline fits) showing U_{sim} are compared to GHP results in Figures 5, 6, and 7.

Figures 5 and 6, corresponding to pane spacings of $L = 17.78$ mm (0.7 in.) and $L = 25.4$ mm (1.0 in.) respectively, show excellent agreement for all slat angles, for both values of ΔT_{bath} and for systems with and without a low-e coating. The discrepancy was less than ±2.7% in all cases except for the two "bumps" found in the GHP measurements at $\phi = -60°$, $L = 25.4$ mm (1.0 in.) and $\Delta T_{bath} = 20°C$ (36°F). These bumps, most readily seen in Figure 2, are unexplained and were found in the measurements of both Garnet (1999) and Huang (2005).

Larger discrepancies can be seen in Figure 7 [$L = 40.01$ mm (1.575 in.)]. If one concludes, based on Figures 5 and 6, that the radiant exchange model is working well then it can also be concluded that the RSL natural convection model ($N = 0.7$) does not work well for the systems with the widest pane spacing. This assertion is supported by the fact that the discrepancies seem in Figure 7 are greater when a low-e

coating is present, the total heat transfer rate being more strongly influenced by convection in these cases.

Mechanisms of Convective Heat Transfer

In the analysis of glazing layers it is clear that convective heat transfer need only be considered between adjacent layers because the fill gas cannot flow from one cavity to the next. However, it is possible for fill gas to flow through a venetian blind and several questions arise because of this difference. Is it necessary to consider convective heat transfer between the two glass surfaces? Is a 1-D model appropriate or is a 2-D model needed? Is there a clearly defined centre-glass region? If so, how big is the edge-glass region?

In a parallel study CFD results were generated (Tasnim 2005) for each of the geometries used in the GHP measurements of Huang (2005). The simulation model was based on the assumptions that the air flow is 2-D and laminar. Several observations were made using the CFD results that support the RSL model.

First, for the $L = 17.78$ mm (0.7 in.) and $L = 25.4$ mm (1.0 in.) cases it was confirmed that, aside from a cyclic
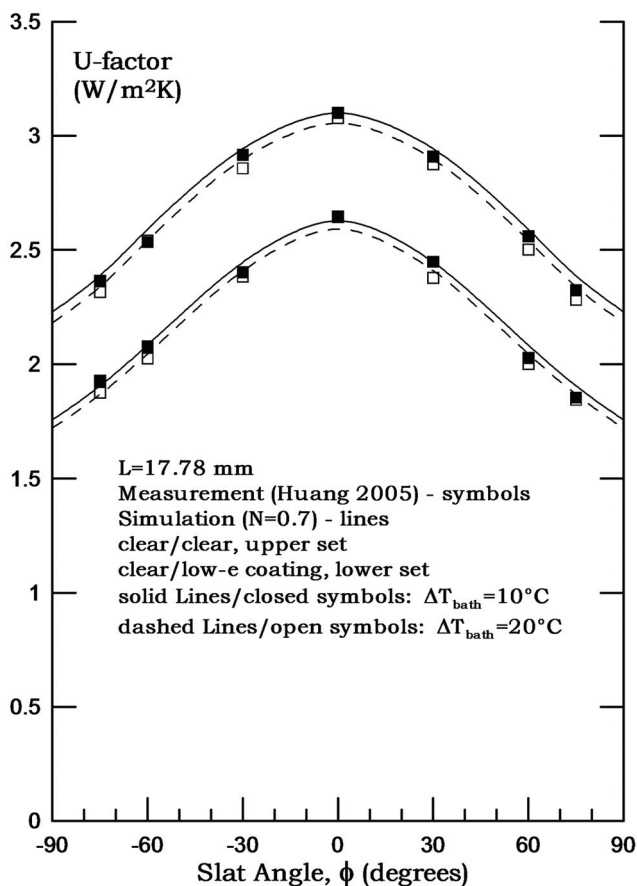
Figure 5 *U-factor versus slat angle, RSL model versus GHP measurement,* L = 17.78 mm (0.7 in.)
Note: Divide U-factor by 5.678 to obtain IP units (Btu/h·ft²·°F).
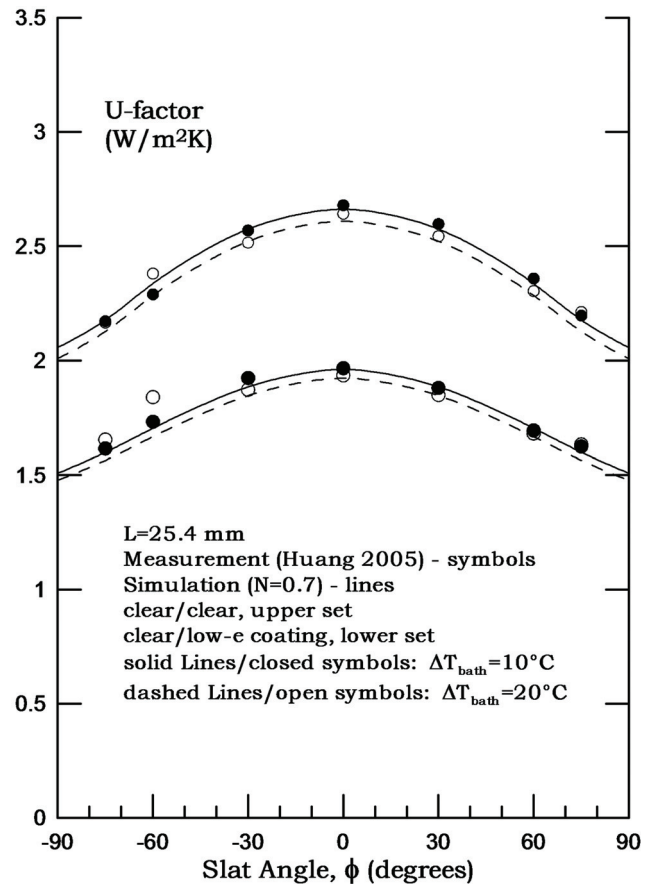
Figure 6 *U-factor versus slat angle, RSL model versus GHP measurement,* L = 25.40 mm (1.0 in.)
*Note: Divide U-factor by 5.678 to obtain IP units (Btu/h·ft²·°F).*
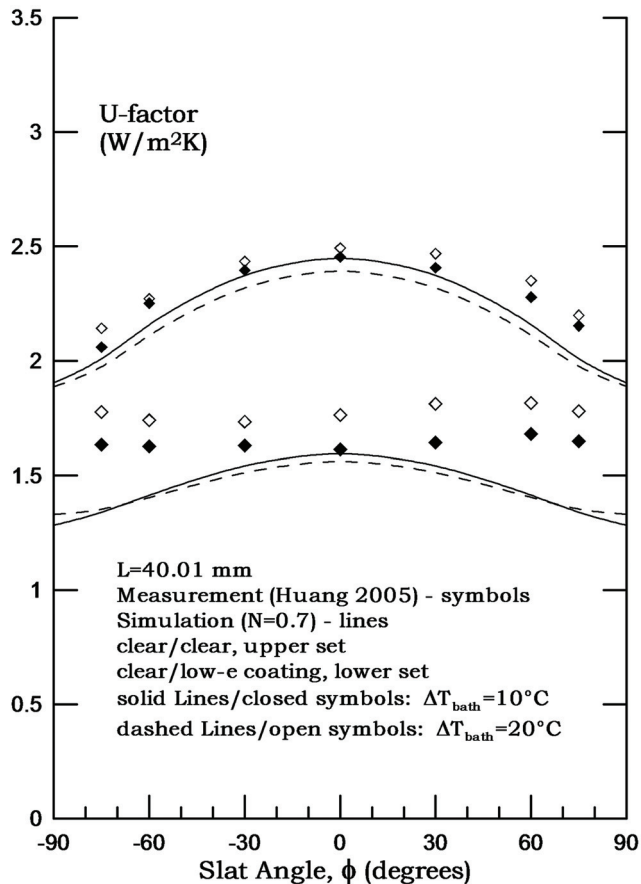
Figure 7 *U-factor versus slat angle, RSL model versus GHP measurement,* L = 40.01 mm (1.575 in.) *Note: Divide U-factor by 5.678 to obtain IP units* $(Btu/h \cdot ft^2 \cdot °F)$.

variation caused by individual slats, the local heat flux is uniform through the centre-glass section of the window. The regions of increased heat flux at the bottom of the warm glazing and reduced heat flux at the top of the warm glazing, caused by the air crossing from one side to the other, are small. These regions easily fall within the 63.5 mm (2.5 in.) distance from the sight line by which the edge-glass region is customarily defined. It can be argued that the presence of the venetian blind will invariably slow the flow by means of blockage and viscous drag. This will also reduce the size of the area over which the crossover flow causes a variation in heat flux. Clearly, it is legitimate to use a 1-D centre-glass model if a venetian blind is present in a glazing cavity.

Figures 8 and 9, from (Tasnim 2005), can be used to illustrate comments that pertain to all of the test cases at $L =$ 17.78 mm (0.7 in.) and $L = 25.4$ mm (1.0 in.). Figure 8 shows a vector plot of the fill-gas flow and Figure 9 shows the corresponding temperature fringe plot, both for one specific condition.

The vector plot shows a primary flow between the slat tips and the adjacent glazing layers. Consider the centre-glass region. Numerical results were examined by Tasnim (2005)
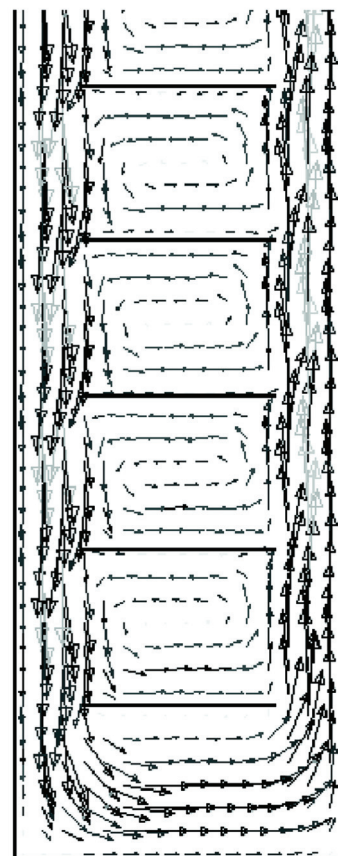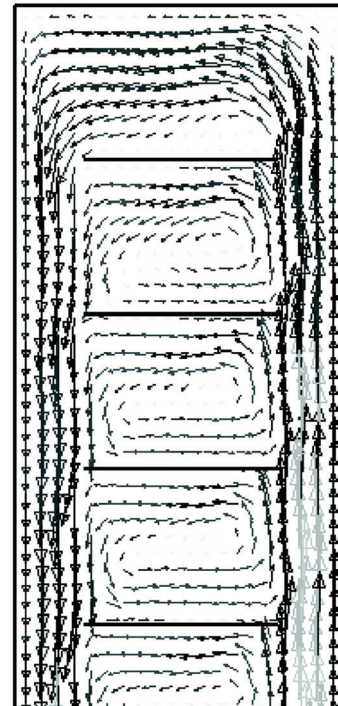
Figure 8 *Flow field for* L = 25.4 mm, f = 0, $T_1 = -10°C$, $T_2 = 25°C$, $T_3 = 7.5°C$ (L = 1.0 in., f = 0, $T_1 = 14°F$, $T_2 = 77°F$, $T_3 = 45.5°F$).
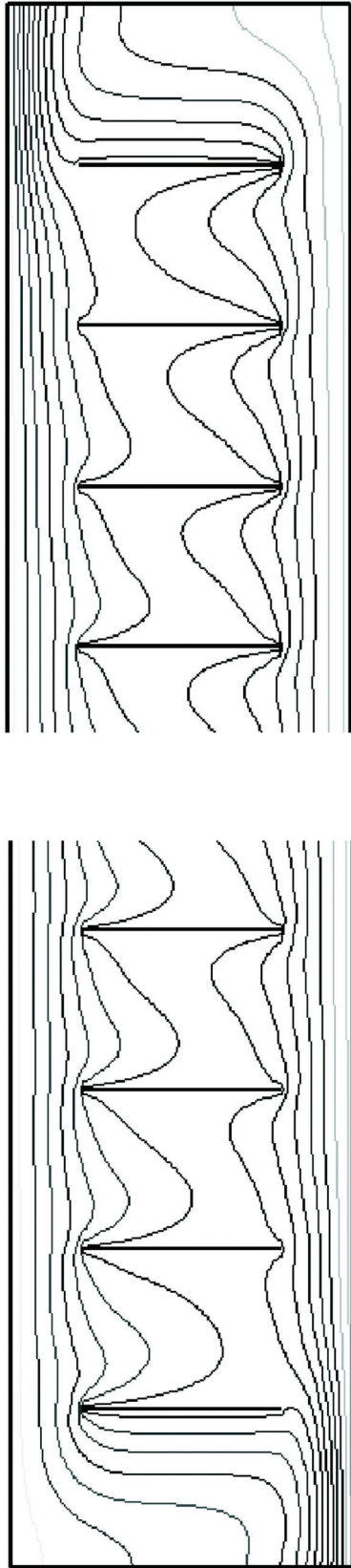
Figure 9   *Temperature fringe plot for* L = 25.4 mm, f = 0,
             T$_1$ = –10°C, T$_2$ = 25°C, T$_3$ = 7.5°C (L = 1.0 in.,
             f = 0, T$_1$ = 14°F, T$_2$ = 77°F, T$_3$ = 45.5°F).

yielding a series of useful observations. The primary flow is very nearly parallel to the vertical cavity wall, making small excursions into the areas between each pair of slats. The net mass flow between adjacent slats (i.e., from one side of the blind to the other) is very small and can be neglected in relation to the primary mass flow. The velocity and temperature profiles of the primary flow, each examined at a surface extending from slat tip to adjacent wall, do not change from one slat tip to the next. This means that the primary flow does not gain or lose energy as the fill gas moves along the vertical wall. Figure 9 shows equally spaced isotherms within the primary flow suggesting that the heat transfer takes place almost entirely by conduction in the direction perpendicular to the fill gas flow. The numerical results show that this is true. The temperature gradient extends a short distance into the area between the slats as if the thermal resistance can be characterized by a conduction layer that is slightly thicker than the true tip-to-glass distance, and this matches the approach used in the RSL model.

Figure 9 also shows that the center or core section of the venetian blind layer is nearly isothermal and this also matches the RSL model in that no thermal resistance was assigned to this portion of the blind layer. The thermal resistance of this core layer is low for two reasons, (1) fill gas circulates in cells between adjacent pairs of slats and (2) the slats are highly conductive. The CFD simulation (Tasnim 2005) was completed by assigning a uniform temperature to the blind slats as if they were very highly conductive. This was done to approximate the slats used in the GHP experiments which were made of aluminum. Plastic slats have a much lower conductivity but it is unlikely that plastic slats would or could be used in this application because of the high temperatures expected in the glazing cavity during times of high solar irradiance.

Applicability of the RSL Model

Under conditions corresponding to each of the GHP experiments the fill gas will move in only one direction in each of the tip-to-glass cavities—upward near the warm glass surface and downward near the cold glass surface. There is a mismatch between this unidirectional flow and the bidirectional flow that exists in the closed, differentially heated, cavity used to mimic each tip-to-glass cavity. Given this mismatch, why does the RSL model work so well? The answer is found in Tables 1 and 2. In all cases with $L = 17.78$ mm (0.7 in.) the Rayleigh number, Ra_{12} or Ra_{23}, does not exceed 1000. With $L = 25.4$ mm (1.0 in.) the Rayleigh number is larger but only slightly exceeds 2500. [Conventional windows are designed to operate at higher Ra, the optimum pane spacing corresponding to Ra $\approx$ 8104 (Hollands et al. 2001, Wright et al. 2006)] These values of Ra are sufficiently low that the calculated Nusselt number, Nu_{12} or Nu_{23}, is equal to unity, or at most 1.01, in every case. A value of Nu = 1 corresponds to pure conduction through the fill gas layer, regardless of whether the flow along the vertical wall is unidirectional or

Table 1. RSL Simulation Results, L = 17.78 mm (0.7 in.), ΔT_{bath} = 20°C (36°F), N = 0.7

Input				RSL Simulation Results						GHP
ε_1	ϕ	T_1	T_3	Ra_{12}	Nu_{12}	Ra_{23}	Nu_{23}	T_2	U_{sim}	U_{meas}
	deg	°C	°C					°C	W/m²·K	W/m²·K
0.84	−90	29.2	11.1	575	1.00	709	1.00	20.4	2.18	—
0.84	−75	29.2	11.1	353	1.00	434	1.00	20.4	2.34	2.32
0.84	−60	29.0	11.3	204	1.00	249	1.00	20.4	2.54	2.54
0.84	−30	28.9	11.5	69	1.00	83	1.00	20.4	2.90	2.86
0.84	0	28.7	11.7	42	1.00	51	1.00	20.4	3.06	3.08
0.84	30	28.9	11.5	71	1.00	86	1.00	20.4	2.90	2.87
0.84	60	29.1	11.3	212	1.00	259	1.00	20.4	2.54	2.50
0.84	75	29.2	11.2	368	1.00	453	1.00	20.5	2.34	2.28
0.84	90	29.2	11.2	600	1.00	740	1.00	20.5	2.18	—
0.164	−90	29.4	11.0	813	1.00	542	1.00	17.7	1.72	—
0.164	−75	29.4	11.0	490	1.00	340	1.00	17.9	1.87	1.87
0.164	−60	29.3	11.0	287	1.00	208	1.00	18.1	2.05	2.02
0.164	−30	29.1	11.2	92	1.00	74	1.00	18.6	2.41	2.38
0.164	0	29.0	11.4	53	1.00	45	1.00	18.8	2.59	2.65
0.164	30	29.1	11.2	92	1.00	74	1.00	18.6	2.41	2.38
0.164	60	29.3	11.0	286	1.00	207	1.00	18.0	2.05	2.00
0.164	75	29.3	10.9	490	1.00	340	1.00	17.8	1.87	1.84
0.164	90	29.3	10.9	812	1.00	542	1.00	17.7	1.72	—

Note: 1) $T_1 \approx 85°F$, $T_3 \approx 52°F$, $T_1 \approx 64$ to 68°F
2) Divide U-factor by 5.678 to obtain IP units (Btu/h·ft²·°F)

Table 2. RSL Simulation Results, L = 25.4 mm (1.0 in.), ΔT_{bath} = 20°C (36°F), N = 0.7

Input				RSL Simulation Results						GHP
ε_1	ϕ	T_1	T_3	Ra_{12}	Nu_{12}	Ra_{23}	Nu_{23}	T_2	U_{sim}	U_{meas}
	deg	°C	°C					°C	W/m²·K	W/m²·K
0.84	−90	29.2	11.1	1745	1.00	2163	1.01	20.5	2.01	—
0.84	−75	29.2	11.1	1250	1.00	1547	1.00	20.4	2.13	2.17
0.84	−60	29.1	11.1	867	1.00	1069	1.00	20.4	2.28	2.38
0.84	−30	29.0	11.3	459	1.00	561	1.00	20.4	2.52	2.52
0.84	0	29.0	11.4	349	1.00	425	1.00	20.5	2.61	2.64
0.84	30	29.1	11.3	454	1.00	556	1.00	20.4	2.52	2.54
0.84	60	29.1	11.2	856	1.00	1054	1.00	20.4	2.28	2.30
0.84	75	29.2	11.1	1260	1.00	1560	1.00	20.4	2.13	2.21
0.84	90	29.2	11.1	1759	1.01	2181	1.01	20.4	2.01	—
0.164	−90	29.5	10.8	2510	1.01	1497	1.00	17.1	1.48	—
0.164	−75	29.5	10.8	1786	1.01	1082	1.00	17.2	1.56	1.65
0.164	−60	29.4	10.8	1248	1.00	771	1.00	17.3	1.67	1.84
0.164	−30	29.4	10.9	648	1.00	428	1.00	17.6	1.85	1.87
0.164	0	29.3	10.9	500	1.00	342	1.00	17.8	1.92	1.94
0.164	30	29.4	10.9	660	1.00	436	1.00	17.6	1.85	1.85
0.164	60	29.4	10.9	1238	1.00	764	1.00	17.3	1.67	1.68
0.164	75	29.4	10.8	1780	1.01	1078	1.00	17.2	1.56	1.63
0.164	90	29.4	10.8	2501	1.01	1491	1.00	17.1	1.48	—

Note: 1) $T_1 \approx 85°F$, $T_3 \approx 52°F$, $T_1 \approx 61$ to 68°F
2) Divide U-factor by 5.678 to obtain IP units (Btu/h·ft²·°F)

Table 3. RSL Simulation Results, *L* = 40.01 mm (1.575 in.), ΔT_{bath} = 20°C (36°F), *N* = 0.7

Input				RSL Simulation Results						GHP
ε_1	ϕ deg	T_1 °C	T_3 °C	Ra_{12}	Nu_{12}	Ra_{23}	Nu_{23}	T_2 °C	U_{sim} W/m²·K	U_{meas} W/m²·K
0.84	−90	29.2	11.0	6854	1.12	8414	1.18	20.4	1.89	—
0.84	−75	29.2	11.0	5053	1.06	6238	1.09	20.4	1.97	2.14
0.84	−60	29.2	11.1	3669	1.03	4532	1.04	20.4	2.11	2.27
0.84	−30	29.1	11.2	2118	1.01	2609	1.01	20.5	2.32	2.43
0.84	0	29.1	11.3	1685	1.00	2072	1.01	20.5	2.39	2.49
0.84	30	29.1	11.2	2124	1.01	2617	1.01	20.5	2.32	2.47
0.84	60	29.2	11.1	3719	1.03	4597	1.05	20.5	2.11	2.35
0.84	75	29.3	11.1	5112	1.06	6314	1.10	20.5	1.98	2.20
0.84	90	29.3	11.1	6936	1.12	8515	1.19	20.5	1.89	—
0.164	−90	29.4	10.9	10,032	1.27	5766	1.08	17.0	1.33	—
0.164	−75	29.4	10.9	7534	1.14	4148	1.04	16.8	1.35	1.78
0.164	−60	29.4	10.9	5538	1.07	2970	1.02	16.8	1.40	1.74
0.164	−30	29.4	10.9	3191	1.02	1757	1.01	16.8	1.51	1.73
0.164	0	29.5	10.9	2547	1.01	1443	1.00	17.0	1.56	1.76
0.164	30	29.5	10.9	3231	1.02	1781	1.01	16.8	1.51	1.81
0.164	60	29.4	10.9	5608	1.07	3013	1.02	16.7	1.40	1.82
0.164	75	29.4	10.9	7583	1.15	4181	1.04	16.8	1.35	1.78
0.164	90	29.4	10.9	10,096	1.27	5812	1.08	17.0	1.33	—

Note: 1) $T_1 \approx 85°F$, $T_3 \approx 52°F$, $T_1 \approx 61$ to 68°F
   2) Divide U-factor by 5.678 to obtain IP units (Btu/h·ft²·°F)

bidirectional, as long as the flow is laminar and the cavity is sufficiently tall.

Table 3 shows appreciably larger values of Ra_{12} and Ra_{23} for the largest pane spacing; the L = 40.01 mm (1.575 in.) case. These larger values of Rayleigh number are caused by the increased tip-to-glass distance. Note that Ra_x is proportional to x^3 (See Equation 12). It is known that the fill gas flow will break into cells and become chaotic and turbulent if Ra is increased sufficiently. These instabilities are of interest to many researchers and are well documented for the tall, vertical gas-filled cavity (i.e., a glazing cavity). See for example (Lartigue et al. 2000, Wright et al. 2006). The same behavior can be expected in the primary flow when a venetian blind is present and convective heat transfer will be augmented by cells and/or turbulence in the primary flow at larger values of Ra. The presence of cells and/or turbulence is consistent with the discrepancies between GHP measurements and the RSL model seen in Figure 7 for the L = 40.01 mm (1.575 in.) case. These discrepancies increase with $|\phi|$ (i.e., larger values of x_{12}, Ra_{12}, x_{23} and Ra_{23}) and are more pronounced when the importance of radiant heat transfer is reduced by the presence of the low-e coating.

The overriding point to be made is that the RSL model works well when the primary fill gas flow is well behaved (i.e., laminar and largely parallel to the vertical cavity walls—free of instabilities). The fill gas flow will behave well as long as the values of Ra_{12} and Ra_{23} (say Ra_{xx}) do not appreciably exceed the values listed in Tables 1 and 2. The critical value of

Ra_{xx} is not readily apparent but it has clearly been exceeded by the configurations with L = 40.01 mm (1.575 in.) and large values of slat angle, ϕ. The values of Ra_{xx} listed in Table 3 for those cases where the RSL model performs poorly fall in the approximate range of $6000 < Ra_{xx} < 10,000$. It is interesting that this is the range of Rayleigh number for which the onset of various instabilities exists in the case of the tall, vertical, rectangular, gas filled cavity (e.g., Lartigue et al. 2000, Wright et al. 2006). Instabilities might be expected at slightly lower values of Ra_{xx} because of the irregular boundary condition at the surface of the venetian blind layer.

The RSL model performs very well for all cases with L = 25.4 mm (1.0 in.). Therefore, the corresponding values of Ra_{xx} listed in Table 2 must correspond to well behaved fill gas flow. The values of Ra_{xx} found in Table 3 [L = 40.01 mm (1.575 in.)] are approximately four times greater and correspond to cases in which the RSL model does not perform so well. The increase in L and the increase in blind-to-glass temperature difference (a fourfold increase) required to increase Ra_{xx} from the levels of Table 2 to the levels of Table 3 are both very unlikely. It is concluded that the RSL model can be safely applied to all situations of practical design. Even in the sunlit case it is unlikely that Ra_{xx} will increase to the level that inaccuracy arises. In fact, if the window is sunlit and the venetian blind is hotter than both glass surfaces a bidirectional flow will exist in both tip-to-glass cavities and it can be argued that the more narrowly confined layers of the bidirectional flow are less susceptible to instability.

Unusual circumstances may trigger uncertainty about the applicability of the RSL model. For example, a very thin venetian blind (small w) may be used. A fill gas other than air may be used; argon will increase Ra by about 25% and krypton will increase Ra by a factor of about 4.5 (Wright and Sullivan 1989). Again, the RSL model will be accurate as long as instabilities are not present in the flow and a check can be made by examining the calculated values of Ra_{12} and Ra_{23}.

Additional simplification follows from the observation that the RSL model works well when the primary fill gas flow is well behaved. When this condition exists the Nu = Nu(Ra) correlation for the tall vertical cavity that is used to mimic the effective tip-to-glass cavity returns Nu = 1.0 or at most Nu = 1.01. Given the need to conserve CPU time during building energy simulations it is recommended that the process be simplified by using $Nu_{12} = Nu_{23} = 1$ in each instance. This leads to the result:

$$h_{12} \text{ or } h_{23} = \frac{2k_{fg}}{L - 0.7 \cdot w \cdot \cos\phi} \quad (18)$$

where k_{fg} is the conductivity of the fill gas in the appropriate tip-to-glass section of the glazing cavity.

This simplification can be expected to produce very little error in the calculation of U-factors and Solar Heat Gain Coefficients (SHGC) for glazing/shading layer arrays. It should be noted that the calculation of SHGC is insensitive to thermal resistance values calculated for individual glazing cavities (Wright 1995) and can also be expected to be insensitive to inaccuracy of the RSL model in the unusual cases corresponding to large values of Ra_{12} and Ra_{23}. It should also be mentioned that an unconventional procedure is required to calculate U-factor and SHGC when any layer in the glazing/shading layer array transmits longwave radiation (Collins and Wright 2006).

CONCLUSIONS

An accurate model, the reduced slat length (RSL) model, has been formulated to quantify the convective heat transfer across a glazing cavity with an enclosed venetian blind. It is possible to account for pane spacing in the range of practical interest, the full range of slat angle, substitute fill gas and the presence of a low-emissivity coating. Coupled with the appropriate model for radiant heat transfer the quantification of total heat transfer within the glazing cavity, and in turn the entire glazing/shading system, can be undertaken.

The RSL model was developed using guarded heater plate measurements and agrees very well with those measurements. Numerical simulation (CFD) results offer support regarding validity and range of applicability of the RSL model. Despite its simplicity the RSL model reflects mechanisms at work in the fluid flow leading to the expectation of accuracy for both night time and sunlit cases. Similarly, it is expected to be accurate in the calculation of both U-factor and SHGC.

The RSL model is exceptionally simple and this feature is of particular value in the context of building energy simulation where CPU time must be used sparingly.

REFERENCES

Bolz, R.E. and G.L. Tuve. 2000. CRC handbook of tables for applied engineering science, 2nd ed. CRC Press, pp. 609.

Carpenter, S. 1992. Thermal performance of window framing systems. *ASHRAE BTECC Conference,* Clearwater, FL.

Collins, M.R. and J.L. Wright. 2006. Calculating centre-glass performance indices of windows with a diathermanous layer. *ASHRAE Transactions* 112(2):22–29.

ElSherbiny, S.M., G.D. Raithby, and K.G.T. Hollands. 1982. Heat transfer by natural convection across vertical and inclined air layers. *Journal of Heat Transfer* 104:96–102.

Finlayson, E.U., D.K. Arasteh, C. Huizenga, M.D. Rubin, and M.S. Reilly. 1993. *WINDOW 4.0: Documentation of calculation procedures*. Energy and Environment Division, Lawrence Berkeley Laboratory, Berkeley, CA.

Garnet, J.M, 1999, Thermal Performance of Windows with Inter-Pane Venetian Blinds. MASc *Thesis*, University of Waterloo, Waterloo, Ontario, Canada.

Garnet, J.M., R.A. Fraser, H.F. Sullivan, and J.L. Wright. 1995. Effect of internal venetian blind on window center-glass U-values. *Proceedings of the Window Innovations Conference*, Toronto, Canada.

Hilsenrath, T., 1955, Thermal properties of gases. National Bureau of Standards *Circular* 564.

Hollands, K.G.T., J.L. Wright, and C.G. Granqvist. 2001. Solar energy—The state of the art—ISES *Position Papers*. James & James Ltd. Ch. 2 (Glazing and Coatings), pp. 29–50.

Hollands, K.G.T. and J.L. Wright. 1983. Heat loss coefficients and effective at products for flat plate collectors with diathermanous covers. *Solar Energy* 30(3):211–216.

Huang, Y.T. 2005. Thermal performance of double glazed windows with inter-pane venetian blinds. MASc. *Thesis*, University of Waterloo, Waterloo, Ontario, Canada.

Huang, Y.T., J.L. Wright, and M.R. Collins. 2006. Thermal resistance of a window with an enclosed venetian blind: Guarded heater plate measurements. *ASHRAE Transactions* 112(2).

Lartigue, B., S. Lorente, and B. Bourret. 2000. Multicellular natural convection in a high aspect ratio cavity: Experi-

mental and numerical results. *International Journal of Heat and Mass Transfer* 43.

Naylor, D. and M. Collins. 2005. Evaluation of an approximate method for predicting the U-value of a window with a between-panes blind. *Numerical Heat Transfer* 47(4):1–18.

Rubin, M., 1982. Calculating heat transfer through windows, *Energy Research* 6:341–349.

Rubin, M., D. Arasteh, and J. Hartmann. 1987. A correlation between normal and hemispherical emissivity for coated window materials. *International Communications in Heat and Mass Transfer* 14.

Shewen, E., K.G.T. Hollands, and G.D. Raithby. 1996. Heat transfer by natural convection across a vertical cavity of large aspect ratio. *Journal of Heat Transfer* 118:993–995.

Tasnim, S.H. 2005. Numerical analysis of convective heat transfer for horizontal, between-the-panes louvred blinds. MASc *Thesis*, Department of Mechanical Engineering, University of Waterloo, Waterloo, Ontario, Canada.

Van Dijk, H.A.L. and J. Goulding, eds. 1996. *Advanced windows information system, WIS reference manual.* TNO Building and Construction Research, Delft, The Netherlands.

Wright, J.L. 1998. Calculating center-glass performance indices of windows. *ASHRAE Transactions* 104(1).

Wright, J.L. 1996. A correlation to quantify convective heat transfer between vertical window glazings. *ASHRAE Transactions* 102(1).

Wright, J.L. 1995. Summary and comparison of methods to calculate solar heat gain. *ASHRAE Transactions* 101(1).

Wright, J.L., 1980, Free convection in inclined air layers constrained by a V-corrugated Teflon film. MASc *Thesis*, University of Waterloo, Mechanical Engineering Department, Waterloo, Ontario, Canada.

Wright, J.L., H. Jin, K.G.T. Hollands, and D. Naylor. 2006. Flow visualization of natural convection in a tall, air-filled vertical cavity, *International Journal of Heat and Mass Transfer*, Vol. 49, Issues 5-6, pp. 889–904.

Wright, J.L. and H.F. Sullivan. 1989. Natural convection in sealed glazing units: A review. *ASHRAE Transactions* 95(1):592–603.

Wright, J.L. and H.F. Sullivan. 1988. Glazing system U-value measurement using a guarded heater plate apparatus, *ASHRAE Transactions* 94(2):1325–1337.

Wright, J.L. and H.F. Sullivan. 1987. Simulation and measurement of windows with low emissivity coatings used in conjunction with Teflon inner glazings. *ISES Solar World Congress*, Hamburg, West Germany. Vol. 4, pp. 3136–3140.

Yahoda, D.S. and J.L. Wright. 2004a. Methods for calculating the effective longwave radiative properties of a venetian blind layer. *ASHRAE Transactions* 110(1).

Yahoda, D.S. and J.L. Wright. 2004b. Heat transfer analysis of a between-panes venetian blind using effective longwave radiative properties. *ASHRAE Transactions* 110(1).